

## Microstructure and non-ohmic properties of ZPCCT-based ceramics

Choon-Woo Nahm

Received: 11 July 2006 / Accepted: 8 August 2006 / Published online: 11 November 2006  
© Springer Science+Business Media, LLC 2006

Zinc oxide doped with several different metal oxides are smart ceramic semiconductors possessing non-ohmic properties, which exhibit abruptly increasing current in accordance with increasing voltage. This non-ohmicity of current–voltage properties is because of the presence of a double Schottky barrier (DSB) formed at active grain boundaries containing many trap states. Owing to highly non-ohmicity, these ceramic devices are used widely in the field of overvoltage protection systems from electronic circuits to electric power systems [1, 2]. ZnO non-ohmic ceramics are generally divided into two categories, called Bi<sub>2</sub>O<sub>3</sub>-based and Pr<sub>6</sub>O<sub>11</sub>-based ceramics, in terms of non-ohmicity-forming oxides. ZnO–Bi<sub>2</sub>O<sub>3</sub>-based ceramics have been mainly studied in various aspects since ZnO non-ohmic ceramics were discovered. Although ZnO–Bi<sub>2</sub>O<sub>3</sub>-based ceramics show excellent non-ohmic properties, Bi<sub>2</sub>O<sub>3</sub> reacts easily with some or many, but not all, of the metals used in preparing multilayer chip non-ohmic ceramics, and it destroys the multilayer structure [3]. And it is reported to have an additional insulating spinel phase, which does not play any role in electrical conduction [3]. Recently, ZnO Pr<sub>6</sub>O<sub>11</sub>-based ceramics have been studied in order to improve a few drawbacks [3] associated with Bi<sub>2</sub>O<sub>3</sub> [4–12].

Nahm et al. reported that Zn–Pr–Co–Cr–R oxide (R = Er, Y, Dy, La)-based ceramics have highly non-ohmic properties [6, 8, 11, 12]. To develop the

non-ohmic ceramics of high performance, it is very important to comprehend the effects of the additives on non-ohmic properties. No study of the effects of Tb<sub>4</sub>O<sub>7</sub> (terbium oxide) on the non-ohmic properties has been reported. In the present study, the effect of Tb<sub>4</sub>O<sub>7</sub> on the microstructure and non-ohmic properties of ZPCCT (ZnO–Pr<sub>6</sub>O<sub>11</sub>–CoO–Cr<sub>2</sub>O<sub>3</sub>–Tb<sub>4</sub>O<sub>7</sub>)-based ceramics was examined.

Reagent-grade raw materials were prepared for ZnO non-ohmic ceramics with composition expression, such as (98.0–*x*) mol% ZnO + 0.5 mol% Pr<sub>6</sub>O<sub>11</sub> + 1.0 mol% CoO + 0.5 mol% Cr<sub>2</sub>O<sub>3</sub> + *x* mol% Tb<sub>4</sub>O<sub>7</sub> (*x* = 0.0, 0.25, 0.5, 0.75, 1.0). Raw materials were mixed by ball milling with zirconia balls and acetone in a polypropylene bottle for 24 h. The mixture was calcined in air at 750 °C for 2 h. The powder was pressed into discs of 10 mm diameter and 2 mm thickness at a pressure of 80 MPa. The discs were sintered at 1350 °C for 1 h. The final samples were 8 mm in diameter and 1.0 mm in thickness. Silver paste was coated on both faces of samples and the electrode was formed by heating at 600 °C for 10 min. The area of electrodes was approximately 0.196 cm<sup>2</sup>.

The surface microstructure was examined by scanning electron microscopy (SEM, Model S2400, Hitachi, Japan). The average grain size (*d*) was determined by the lineal intercept method [13]. The compositional analysis of the selected areas was determined by an attached energy dispersion X-ray analysis (EDX) system. The crystalline phases were identified by powder X-ray diffraction (XRD, Model D/max 2100, Rigaku, Japan) with CuK<sub>α</sub> radiation. The sintered density ( $\rho$ ) was measured by the Archimedes method. The current–voltage (*I*–*V*) characteristics of ZPCCT-based ceramics

C.-W. Nahm (✉)  
Department of Electrical Engineering, Dongeui University,  
Busan 614-714, Korea  
e-mail: cwnahm@deu.ac.kr

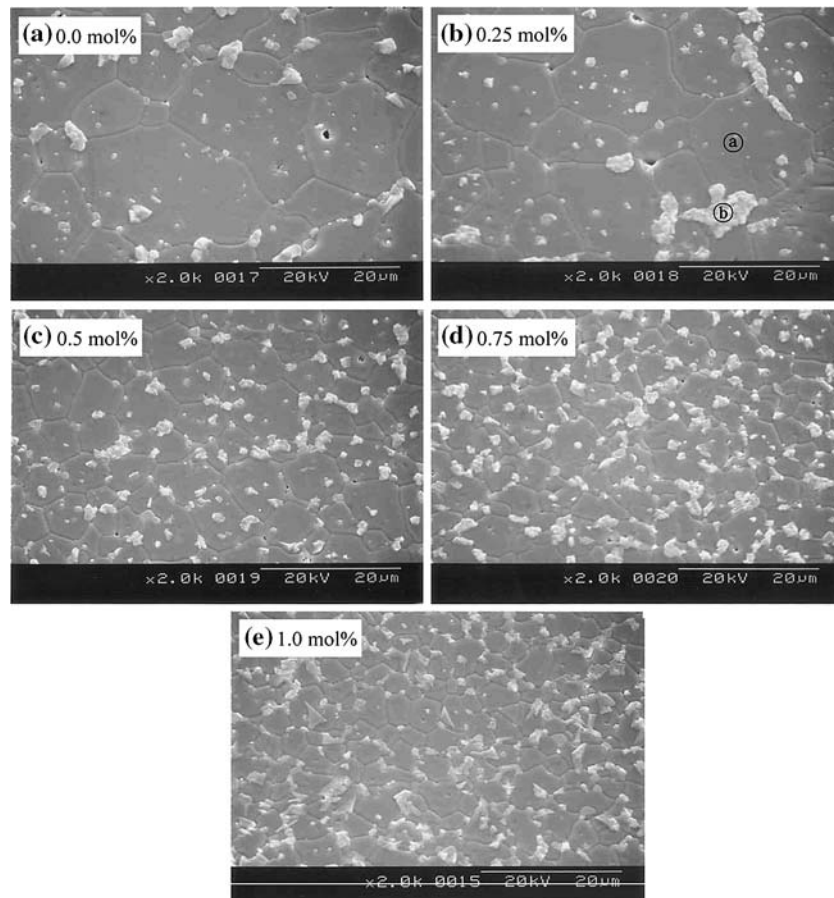
were measured using an I–V source/measure unit (Keithley 237). The breakdown voltage ( $V_B$ ) was measured at  $1.0 \text{ mA/cm}^2$  and the leakage current ( $I_L$ ) was measured at 80 % of breakdown voltage. In addition, the non-ohmic coefficient ( $\alpha$ ) is defined by the empirical law,  $J = K \cdot E^\alpha$ , where  $J$  is the current density,  $E$  is the applied electric field, and  $K$  is constant. The  $\alpha$  was determined in the current density range  $1.0 \text{ mA/cm}^2$  to  $10 \text{ mA/cm}^2$ , by  $\alpha = 1/(\log E_2 - \log E_1)$ , where  $E_1$  and  $E_2$  are the electric field corresponding to  $1.0 \text{ mA/cm}^2$  and  $10 \text{ mA/cm}^2$ , respectively.

Figure 1 shows the SEM micrographs of ZPCCT-based ceramics for different  $\text{Tb}_4\text{O}_7$  contents. The microstructure consisted of primary phase ZnO grain, and secondary phase intergranular, which are Pr- and Tb-rich phases as determined by XRD analysis, as shown in Fig. 2. Figure 3 shows a distribution of Tb by EDX. No Tb peak into ZnO grain was found within the EDX detection limit. It is assumed that this is attributed to the ionic radius difference for Zn. Added  $\text{Tb}_4\text{O}_7$  as well as  $\text{Pr}_6\text{O}_{11}$  was segregated to grain boundaries and nodal points, and Pr- and Tb-oxide were found to coexist in the grain boundaries and the nodal points as if they were a single phase. The

sintered density increased from  $5.73$  to  $5.85 \text{ g/cm}^3$  in accordance with increasing  $\text{Tb}_4\text{O}_7$  contents. There is nearly no porosity through the surface microstructure. Non-ohmic ceramics added with other earth metal oxides hardly provide both high sintered density and highly non-ohmicity [6, 8, 11, 12]. Therefore, the high sintered density is very important for high energy capability. The average grain size was greatly decreased from  $13.1$  to  $5.0 \mu\text{m}$ . Therefore the densification is found to be enhanced by the addition of  $\text{Tb}_4\text{O}_7$ . The detailed microstructural parameters are summarized in Table 1.

Figure 4 shows the  $E$ – $J$  characteristics of the ZPCCT-based ceramics for different  $\text{Tb}_4\text{O}_7$  contents. The curves show the conduction characteristics divide into two regions: ohmic region before breakdown field and non-ohmic region after breakdown field. The sharper the knee of the curves between the two regions, the better the non-ohmic properties. On adding more  $\text{Tb}_4\text{O}_7$ , the knee gradually becomes more pronounced and the non-ohmic properties are enhanced. Therefore, the addition of  $\text{Tb}_4\text{O}_7$  seems to remarkably enhance non-ohmic properties. The breakdown voltage ( $V_B$ ) greatly increased from  $102.6$  to

**Fig. 1** Micrographs of ZPCCT-based ceramics for different  $\text{Tb}_4\text{O}_7$  contents



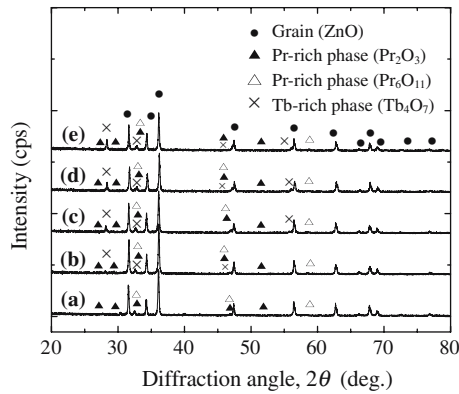


**Fig. 2** XRD patterns of ZPCCT-based ceramics for different  $\text{Tb}_4\text{O}_7$  contents; (a) 0.0 mol%, (b) 0.25 mol%, (c) 0.5 mol%, (d) 0.75 mol%, and (e) 1.0 mol%

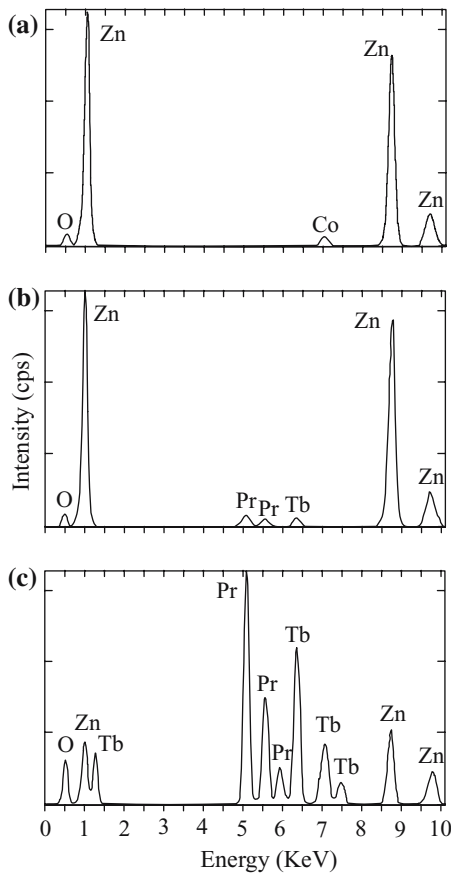


**Fig. 3** EDX analysis of ZPCCT-based ceramics; (a) ZnO grain, (b) grain boundary, and (c) intergranular layer

651.4 V/mm in accordance with increasing  $\text{Tb}_4\text{O}_7$  content. The samples added with  $\text{Tb}_4\text{O}_7$ , more than 0.75 mol%, provide a very high breakdown voltage of 500 to 600 V/mm per unit thickness. This is very important for high voltage non-ohmic ceramics with compact size. The increase of  $V_B$  in relation to

**Table 1** Microstructure and  $I$ – $V$  characteristic parameters for different  $\text{Tb}_4\text{O}_7$  contents

$\text{Tb}_4\text{O}_7$ content (mol%)	$d$ ( $\mu\text{m}$ )	$\rho$ ( $\text{g}/\text{cm}^3$ )	$V_B$ (V/mm)	$V_b$ (V)	$\alpha$	$I_L$ ( $\mu\text{A}$ )
0.00	13.1	5.73	102.6	1.3	8.9	40.1
0.25	10.1	5.75	140.8	1.4	18.6	4.6
0.50	7.3	5.80	299.1	2.2	31.7	1.7
0.75	5.1	5.82	588.2	3.0	35.9	1.7
1.00	5.0	5.85	651.4	3.3	42.0	3.0

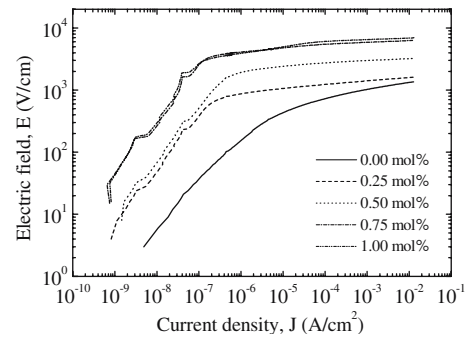


**Fig. 4**  $E$ – $J$  characteristics of ZPCCT-based ceramics for different  $\text{Tb}_4\text{O}_7$  contents

increasing  $\text{Tb}_4\text{O}_7$  content can be explained by the increase in the number of grain boundaries owing to the decreases in the average ZnO grain size. The samples added with  $\text{Tb}_4\text{O}_7$ , less than 0.25 mol%, exhibited much lower  $V_b$  value than the general value of 2–3 V. These samples below 2.0 V generally exhibit very poor non-ohmic properties.

Figure 5 shows the variation of the non-ohmic coefficient ( $\alpha$ ) and the leakage current ( $I_L$ ) of the ZPCCT-based ceramics as a function of  $\text{Tb}_4\text{O}_7$  con-

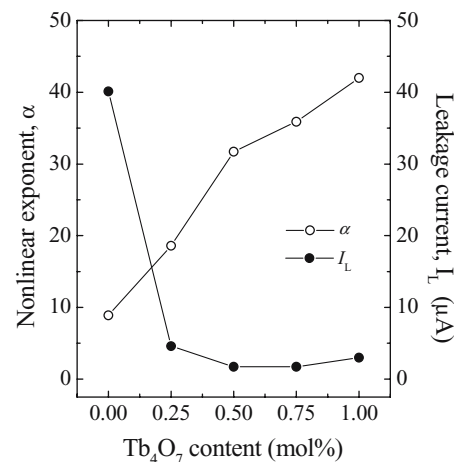


**Fig. 5** Non-ohmic coefficient and leakage current of ZPCCT-based ceramics as a function of  $\text{Tb}_4\text{O}_7$  contents

tent. The  $\alpha$ -value of the samples without  $Tb_4O_7$  was only 8.9, whereas the  $\alpha$  value of the samples added with  $Tb_4O_7$  increased linearly in the range of 18.6–42.0. On the other hand, the  $I_L$  value of the samples without  $Tb_4O_7$  was as much as 40.1  $\mu A$ , whereas the  $I_L$  value of the samples added with  $Tb_4O_7$  decreased abruptly in the range of 1.7–4.6  $\mu A$ . It can be seen that the variation of  $I_L$  shows the inverse relationship to the variation of  $\alpha$  in relation to  $Tb_4O_7$  content. Therefore, it was found that the addition of  $Tb_4O_7$  to the quaternary system  $ZnO-Pr_6O_{11}-CoO-Cr_2O_3$  remarkably improves the  $I-V$  characteristics, namely, it makes the non-ohmic coefficient higher and the leakage current smaller. It is clear that the  $\alpha$  and  $I_L$  value was strongly influenced by the  $Tb_4O_7$  content. The detailed  $I-V$  parameters are summarized in Table 1.

In summary, the ZPCCT-based ceramics exhibited not only high densification but also good non-ohmic properties. Therefore, it is expected that the ZPCCT-based ceramics would be applied to the non-ohmic

materials. A more detailed study will be reported in a forthcoming paper.

## References

1. Levinson LM, Pilipp HR (1986) Amer Ceram Soc Bull 65:639
2. Gupta TK (1990) J Amer Ceram Soc 73:1817
3. Lee YS, Tseng TY (1992) J Amer Ceram Soc 75:1636
4. Alles AB, Burdick VL (1991) J Appl Phys 70:6883
5. Lee Y-S, Liao K-S, Tseng T-Y (1996) J Amer Ceram Soc 79:2379
6. Nahm C-W (2001) Mater Lett 47:182
7. Nahm C-W (2002) J Mater Sci Lett 21:201
8. Nahm C-W (2003) Mater Lett 57:1317
9. Nahm C-W, (2003) Solid State Commun 127:389
10. Nahm C-W, Park J-A, Kim M-J, Shin B-C (2004) J Mater Sci 39:307
11. Nahm C-W (2004) J Mater Sci 39:307
12. Nahm C-W (2005) J Mater Sci 40:6307
13. Wurst JC, Nelson JA (1972) J Amer Ceram Soc 55:109